J Therm Anal Calorim (2010) 99:459–464
DOI 10.1007/s10973-009-0168-3

Obtaining of $Ni_{0.65}Zn_{0.35}Fe_2O_4$ nanoparticles at low temperature starting from metallic nitrates and polyols

Mircea Stefanescu · Marcela Stoia · Oana Stefanescu · Paul Barvinschi

Received: 18 February 2009 / Accepted: 29 April 2009 / Published online: 28 August 2009

Abstract This article presents a study on obtaining Ni, Zn ferrite starting from Fe(III), Ni (II), Zn (II) nitrates and some polyols: 1,2-propane diol, 1,3-propane diol and glycerol. While heating, a redox reaction takes place between nitrate anion and polyol, with formation of carboxylate type precursors. The obtained precursors have been investigated by thermal analysis, FT-IR spectrometry and atomic absorption spectroscopy. The thermal decomposition of the synthesized precursors up to 350 °C leads to the formation of Ni, Zn ferrite as unique phase, evidenced by XRD. The average diameter of the ferrite crystallites, estimated from XRD data, takes values within the range 20–50 nm, depending on the annealing temperature. Transmission Electron Microscopy has evidenced the obtaining of spherical, agglomerated nanoparticles. The magnetic properties of the synthesized samples, measured in cvasistatic magnetic field (50 Hz) are characteristic for the Ni, Zn ferrite nanoparticles, with narrow hysteresis cycle and values of the saturation magnetization <70 emu/g.

Keywords Carboxylates · Ferrite · Polyols · Thermal analysis

Introduction

The current tendency of using oxidic materials as nanoparticles leaded to the permanent development of new unconventional synthesis methods [1–4]. This is due to the different properties of the nanomaterials compared to the bulk material.

The thermal conversion of precursors is a frequently used unconventional synthesis method. Coordination compounds with carboxylate type ligands are an important class of nanomaterial precursors. By thermal decomposition of these precursors, depending on the systems composition and thermal treatment, magnetic materials, catalysts, pigments and luminophores may be obtained [5–9].

The Ni–Zn ferrite represents a material of high technological importance and it has been the subject of many scientific papers [10–13]. The Ni–Zn ferrite belongs to the class of soft ferrimagnetic materials, with low magnetic coercivity and resistivity, properties that make it an excellent material with different applications in telecommunications, electronics, microwaves devices, magnetic heads for reading digital equipments of high speed [14–19].

In our previous studies we have obtained the Ni, Zn ferrite by thermal decomposition of heteropolynuclear coordination compounds formed in the redox reaction between NO_3^- (from Fe(III), Ni(II), Zn(II) nitrates) and ethylene glycol (EG) [20].

This article presents a study on obtaining Ni–Zn ferrite nanoparticles using other polyols: 1,2-propane diol (1,2 PG), 1,3-propane diol (1,3 PG) and glycerol (GL) as reducing agents in the redox reaction with NO_3^- ions (from the mixture of $Fe(NO_3)_3$, $Ni(NO_3)_2$ and $Zn(NO_3)_2$). We studied the redox reaction between each polyol and the mixture of

---

M. Stefanescu (✉) · M. Stoia · O. Stefanescu
Faculty of Industrial Chemistry and Environmental Engineering, “Politehnica” University, P-ta Victoriei no.2, 300006 Timisoara, Romania
e-mail: mircea.stefanescu@chim.upt.ro

P. Barvinschi
Faculty of Physics, West University, Bv. V. Parvan no. 4, 300223 Timisoara, Romania

metallic nitrates and the thermal decomposition of these precursors in order to obtain the $Ni_{0.65}Zn_{0.35}Fe_2O_4$ nanopowders at low temperatures. Magnetic measurements performed on the obtained powders have evidenced superparamagnetic behavior characteristic to magnetic Ni–Zn ferrite nanoparticles.

Experimental

Analytically pure 1,2-propane diol, 1,3-propane diol, glycerol and $Fe(NO_3)_2 \cdot 9 \cdot H_2O$, $Ni(NO_3)_2 \cdot 6 \cdot H_2O$, $Zn(NO_3)_2 \cdot 6 \cdot H_2O$ (supplied by Merck) were used as reagents without further purification.

$Ni_{0,65}Zn_{0,35}Fe_2O_4$ ferrite was synthesized using a molar ratio polyol: $NO_3^- = 1{:}1$. The metallic nitrates were solved in the corresponding polyol amount and diluted with distilled water to 3 mol/L of NO_3^- concentration. The obtained solutions were carefully heated on water bath, when the redox reaction took place between nitrate ions and polyol, forming a viscous reaction product containing the corresponding metallic carboxylates. By maintaining the product at 130 °C, we have obtained a solid, dried product, which was washed with acetone in order to remove the polyol excess.

Thus, there were synthesized forerunners starting from the mixture of metallic nitrates with different polyols: D1 (with 1,2PG), D2 (with 1,3PG) and D3 (with GL).

The development of the redox reaction between metallic nitrates and polyols was investigated by thermal analysis. The obtained forerunners have been characterized by FT-IR spectrometry, thermal analysis and absorption atomic spectroscopy (AAS).

The obtained products D1, D2, D3 have been annealed at different temperatures in order to obtain $Ni_{0,65}Zn_{0,35}Fe_2O_4$ ferrite as unique phase. The obtained powders have been characterized by XRD, TEM and magnetic measurements.

Thermal analysis was performed on a 1500D MOM Budapest Derivatograph. The heating was achieved in static air, up to 500 °C, with a heating rate of 5 °C min^{-1}, on Pt plates using α-Al_2O_3 as inert material. The FT-IR spectra were acquired over the range 400–4000 cm^{-1}, in KBr pellets, with a JASCO 430 FT-IR spectrometer. AAS analysis was performed with Aanalyst 800-Perkin Elmer. Phase analysis was achieved with D8 Advance-Bruker AXS diffractometer (samples obtained at 350 and 800 °C) and with Dron 3 diffractometer (samples obtained at 400 °C) using Cu-K_α radiation ($\lambda_{Cu} = 1,\ 54056$ Å). The TEM images were performed on a JEOL JEM 101 microscope. The behavior in external magnetic field of the obtained nanocomposites was performed with an installation equipped with a data acquisition system.

Results and discussion

Former studies on the redox reaction between metallic nitrates and diols (EG, 1,2 PG, 1,3 PG) [9, 21] have shown that diols oxidation products (carboxylate, hydrocarboxylate, dicarboxylate anions) coordinate to the metallic ions forming coordination compounds.

The ligands nature and the formed complex depend on the used polyol, on the metallic cations nature and on the work conditions (concentration, acidity, heating conditions, molar ratio NO_3^-: polyol). The studies on the redox reaction between the NO_3^- ion and different polyols have shown that only the –H_2C–OH (primary) groups are oxidized in these conditions [21].

1,2-propanediol is oxidized by NO_3^- ions to the lactate anion (CH_3–CH_2(OH)–COO^-) [24], while 1,3-propane diol may oxidize to the 3-hidroxy-propionate anion (HO–CH_2–CH_2–COO^-) or to the malonate anion ($^-$OOC–CH_2–COO^-) [21]. In case of glycerol, due to the three –OH groups, the oxidation process is complex and leads to different oxidation products (glyceric acid, glyceric aldehyde, hydroxymalonic acid). Generally, it is difficult to obtain a unitary oxidation product of glycerol [22]. The anions resulted in the redox reaction, coordinate to the metallic ions present in the system, forming coordination compounds.

The redox reaction between metallic nitrates mixture and polyol was studied by thermal analysis, by deposing the reactant mixture as film on Pt plates. Figure 1 presents the obtained DTA curves.

In each case, two exothermic effects were registered on the DTA curve. The first exothermic effect, in the range 60–90 °C, corresponds to the redox reaction NO_3^--polyol with formation of coordinative compounds between the oxidation products of the polyols and the metallic ions. The second exothermic effect, in the range 250–350 °C, corresponds to the oxidative decomposition of the formed precursors. Based on thermal analysis data, we have

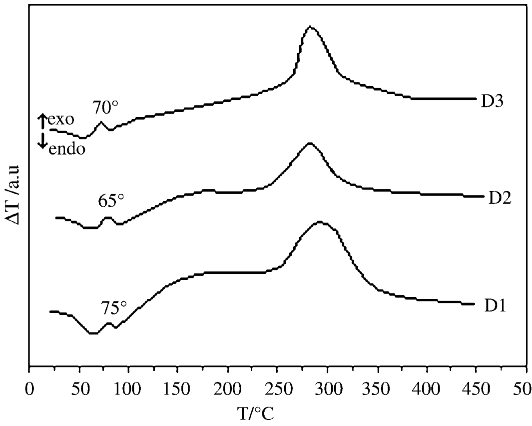

Fig. 1 DTA curves of the mixtures Fe(III), Ni(II), Zn (II) nitrates–polyols: D1 (1,2 PG), D2 (1,3 PG), D3 (GL)

established 130 °C as optimal synthesis temperature for the ferrite precursors D1, D2, D3.

Atomic absorption spectrometry was used in order to verify the molar ratio of the three metallic ions: Fe:Ni:Zn, in each precursor (Table 1). The results showed that the metallic ions are present in the precursors in molar ratios close to the introduced one (Fe:Ni:Zn = 2: 0.65:0.35).

The formation of the coordination compounds between metallic ions and the carboxylate ligands was evidenced by FT-IR spectrometry. Table 2 presents the bands of the characteristic FT-IR spectra and their assignment for D1, D2, D3.

The strong band at 1620 cm^{-1} assigned to the vibration v_{as} (COO^-) of the coordinated carboxylate group [23], the band at 1360 cm^{-1} assigned to v_s (COO^-) [24] present in all spectra evidenced the existence of the carboxylate group coordinated to the metallic cations in all synthesized precursors. In case of precursors D1 and D3 synthesized with 1,2 PG and GL, in the spectra appears at 1090 cm^{-1} a supplementary band attributed to v(C-OH) vibrations, characteristic for the secondary –OH group [21]. The value of ~260 cm^{-1} for the difference $\Delta = v_{as}(COO^-) - v_s(COO^-)$, greater than the one corresponding to the sodium salts (sodium lactate, sodium malonate, sodium glycerate, (between 170–200 cm^{-1}) suggests that the carboxylate group coordinates in a monodentate way [26].

Figures 2, 3, 4 present the TG and DTA curves registered for the synthesized precursors D1, D2 and D3.

In the range 20–150 °C, the profiles of the TG and DTA curves are similar, for all precursors, with little mass loss, and no significant thermal effects, due to the dehydration process. In the range 150–350 °C the oxidative decomposition of the metallic complexes takes place, in several steps. Our studies on the thermal decomposition of the homonuclear compounds synthesized from each metallic nitrate with each polyol showed that they decompose in a single step, with an exothermic effect, in the ranges: 200–250 °C for Fe(III) compounds [27], 260–300 °C for Ni(II) compounds and 290–350 °C in case of Zn(II) compounds. The evolution of the thermal curves in the range 200–350 °C presented in Figs. 2,3,4 suggests the formation of a homogenous mixture of Fe(III), Ni(II) and Zn(II) homonuclear complexes. The thermal effects of the decomposition of these compounds overlap, depending on the ligands nature.

In case of precursors D1 (Fig. 2) and D2 (Fig. 3) the thermal decomposition of Fe(III) and Ni(II) carboxylates takes place up to 260 °C. Both, mass losses and thermal effects of these steps partially overlap. The decomposition of the Zn(II) carboxylate takes place in the range 260–320 °C with a weak exothermic effect.

Table 1 Results of AAS analysis for the synthesized precursors D1, D2, D3

Precursor	Mass percent/wt%			Molar ratio Fe:Ni:Zn
	Fe	Ni	Zn	
D1	21.2 ± 0.8	7.7 ± 0.5	4.1 ± 0.3	(2.00 ± 0.07):(0.69 ± 0.05):(0.33 ± 0.02)
D2	16.2 ± 0.4	5.3 ± 0.3	3.4 ± 0.1	(2.00 ± 0.06):(0.64 ± 0.03):(0.38 ± 0.02)
D3	12.5 ± 0.2	4.3 ± 0.3	2.7 ± 0.1	(2.00 ± 0.04):(0.67 ± 0.05):(0.39 ± 0.01)

Table 2 FT-IR bands corresponding to the precursors D1, D2, D3

Wavenumbers/cm^{-1}			Assignment
D1	D2	D3	
3393	3403	3395	υ(OH) assoc.; [21]
2979, 2936, 2820	2954, 2887	2940, 2880	υ(CH) [23]
1620	1619	1625	$\upsilon_{as}(COO^-)$ [23, 24]
1359	1359	1360	$\upsilon_s(COO^-)$ [24]
1316	1317	1316	υ(C–O) + δ(OCO) [21]
1120	1241	–	δ(OH) ROH + υ(C–O) [25]
1085		1092	υ(C–OH) [21]
1048	1059	1045	υ(C–OH); υ(OH) bridge [21]
920	930	920	υ(C–C) [23]
825, 803	819, 806	821	δ(OH) R–OH [30]; $\rho(CH_2)$ [21]
684	691	674, 663	$\rho(H_2O)$ [24]; υ(M-O) [23]
610,591			δ(OCO) [25]
489	489	488	υ(M–O) [21]

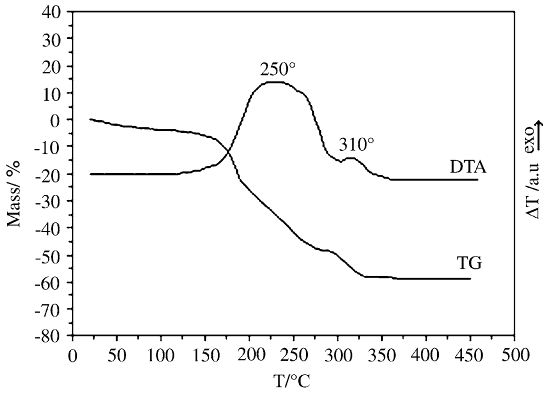

Fig. 2 TG and DTA curves of precursor D1

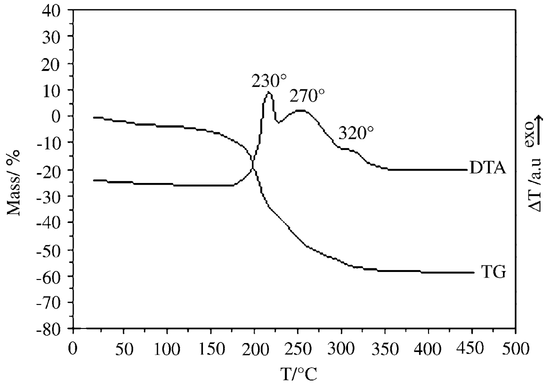

Fig. 3 TG and DTA curves of precursor D2

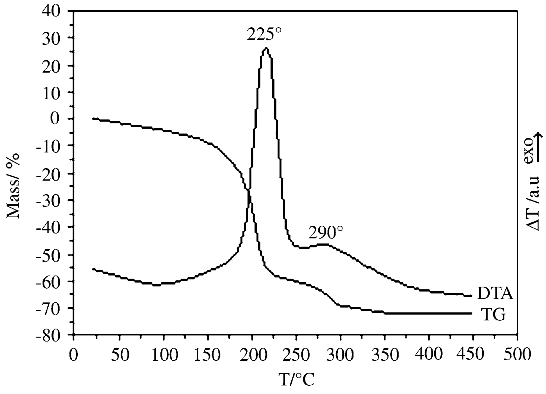

Fig. 4 TG and DTA curves of precursor D3

In case of precursor D3 (Fig. 4), synthesized with glycerol, the mass loss takes place in a single step, in the range 150–230 °C, associated to a single exothermic effect at 225 °C. This can due to the oxidative decomposition of the oxidation products mixture resulted in the redox reaction between glycerol and Fe(III), Ni(II) nitrates. The decomposition of the corresponding Zn compounds takes place in the range 250–300 °C with a low exothermic effect.

All synthesized precursors decompose up to 350 °C with formation of the mixed oxidic system. XRD analysis

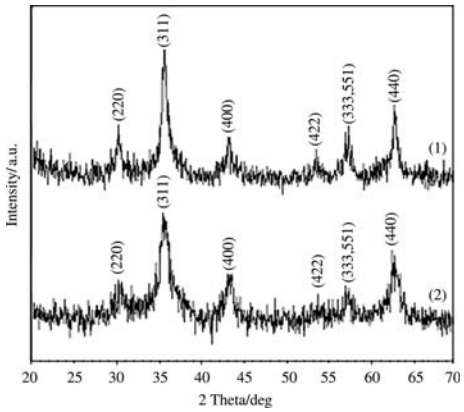

Fig. 5 XRD patterns of the thermal decomposition residues of (1) D2 and (2) D3 at 350 °C

of the residues at 350 °C resulted at thermal decomposition of the synthesized precursors, evidenced Ni, Zn ferrite as unique phase (Fig. 5). The formation of Ni, Zn ferrite at low temperatures, by thermal decomposition of metallic carboxylates is due to the enhanced reactivity of the oxides mixture (γ-Fe_2O_3, NiO, ZnO). This can be explained by the reducing atmosphere generated in situ during the oxidative decomposition of the organic ligands. These conditions promote the reduction of Fe(III) to Fe(II) and Ni(II) to Ni(0) followed by the re-oxidation to highly reactive γ-Fe_2O_3 [27] and NiO which react with ZnO leading to Ni, Zn ferrite formation at 350 °C.

In order to obtain Ni–Zn ferrite powders, the precursors D1, D2, D3 were annealed at 400, 600 and 800 °C, for 3 h. The XRD patterns of the samples annealed at 400 °C (Fig. 6) evidence only the diffraction peaks characteristic to the spinel phase of Ni–Zn ferrite. The crystallization degree increases with the annealing temperature (600, 800 °C). At 800 °C the Ni, Zn ferrite appears well crystallized in all cases (Fig. 7).

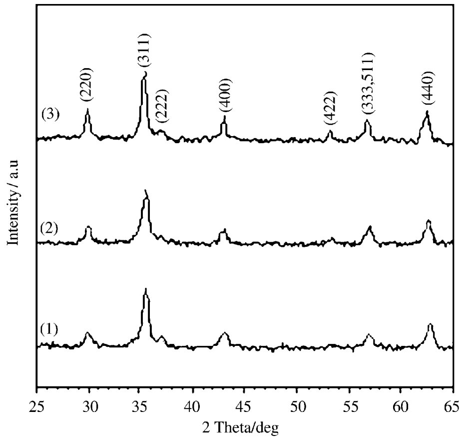

Fig. 6 XRD patterns of the samples annealed at 400 °C: (1) D1, (2) D2, (3) D3

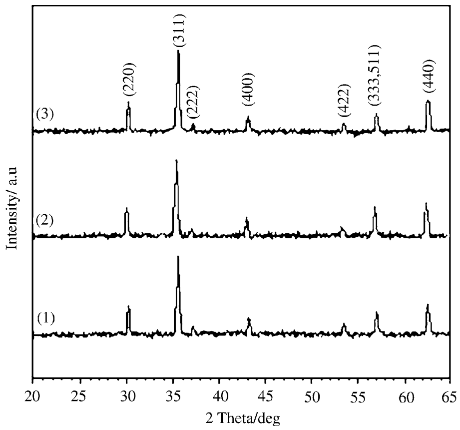

Fig. 7 XRD patterns of the samples annealed at 800 °C: (1) D1, (2) D2, (3) D3

From the XRD patterns of the samples D1, D2, D3 annealed at 800 °C we have estimated the average diameter (d) of the ferrite nanocrystallites as well as the network parameter (a_0). Because the Ni, Zn ferrite have a cubic structure, the lattice parameter can be determined using the plane-spacing equation $a = d_{hkl}(h^2 + k^2 + l^2)^{1/2}$, where d_{hkl} is measured from the $\sin\theta_{hkl}$ value in the Bragg equation $2d_{hkl}\sin\theta_{hkl} = \lambda$ for each reflection having the Miller indices (*hkl*). The true value of the lattice parameter (a_o) is obtained by extrapolating the straight line of lattice parameter, for each θ_{hkl}, versus an extrapolation function of θ to the value corresponding to 0 (i.e. for $\theta = 90^{\circ}$) [28]. The extrapolation function used in our work was $\cos^2\theta/\sin\theta$, taking into consideration the diffraction peaks of the following crystal-lattice planes: (220), (311), (400), (422), (511) and (440). The crystallites size was calculated using the Scherrer relation, after the substraction of instrumental broadening and taking into consideration the strain in the material. The size of the network parameter (a_o) and the average crystallites size (D_{av}) for the samples annealed at 800 °C is presented in Table 3.

The network parameter values for the obtained $Ni_{0,65}Zn_{0,35}Fe_2O_4$ powders (Table 3) are comprised between the value $a = 8.339$ Å corresponding to $NiFe_2O_4$ (JCPDS 10-0325) and $a = 8.441$ Å corresponding to $ZnFe_2O_4$ (JCPDS 22-1012), in agreement with the JPCDS-08-0234 for (Ni, Zn)Fe_2O_4 ($a = 8.399$ Å) [29].

Table 3 Network parameter (a_o) and average crystallite size (D_{av}) calculated for Ni, Zn ferrite obtained at 800 °C

Parameter	Samples		
	D1	D2	D3
a_o (Å)	8.389 ± 0.004	8.387 ± 0.003	8.385 ± 0.002
D_{av} (nm)	47 ± 8	40 ± 7	47 ± 6

All Ni–Zn ferrite powders, obtained by annealing the ferrite precursors at 400, 600, and 800°C, presented characteristic magnetic properties. Figure 8 presents the magnetization curves at room temperature of the Ni–Zn nanoferrite samples obtained at 800 °C. The values of the saturation specific magnetization ($65 \div 70$ emu/g) registered for Ni, Zn ferrite obtained from the precursors D1, D2 and D3 suggest that, at this temperature, the ferrite nanocrystallites are agglomerated.

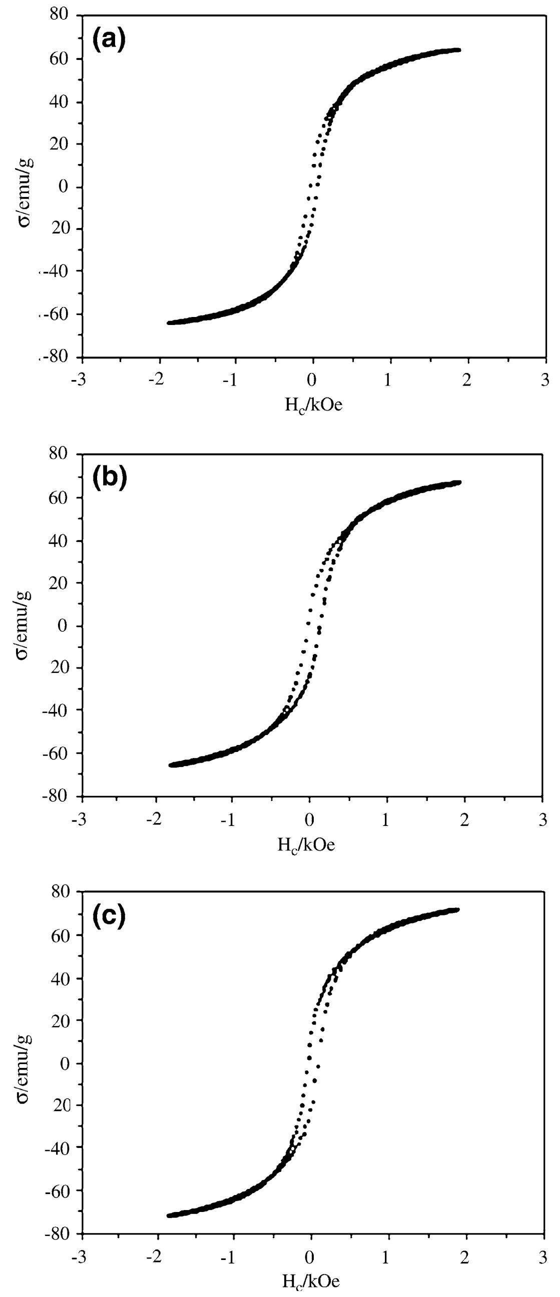

Fig. 8 Magnetization curves of the samples annealed at 800 °C: **a** D1, **b** D2, **c** D3

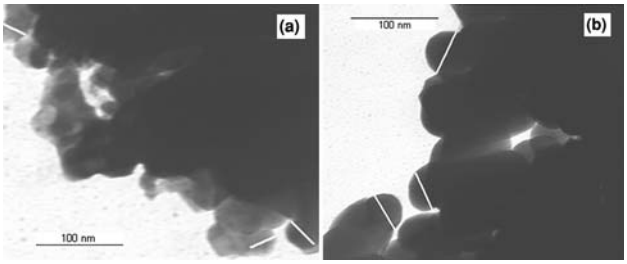

Fig. 9 TEM images of the samples D1 (**a**) and D2 (**b**) annealed at 800 °C

Figure 9 presents the TEM images obtained for the samples D1 and D2, annealed at 800 °C. From the TEM images we can observe that the particles are nearly spherical, with diameters below 100 nm. These nanoparticles are agglomerated and they are difficult to disperse.

Conclusions

Single-phase nanosized $Ni_{0.65}Zn_{0.35}Fe_2O_4$ ferrite has been prepared at low temperature (350 °C) by thermal decomposition of the carboxylate type precursors formed in the redox reaction between the mixture of metallic nitrates and different polyols (1,2 PG, 1,3 PG, GL). All synthesized precursors, thermally decompose up to 350 °C, when Ni, Zn ferrite forms, due to the enhanced reactivity of the individual metallic oxides. By further thermal treatments, at higher temperatures, Ni, Zn ferrite forms as nanocrystallites with characteristic magnetic properties. In conclusion, this precursors (metallic carboxylates) obtained in the redox reaction between the corresponding metallic nitrates and the studied polyols allow the preparation of nanosized nickel–zinc ferrite at low temperature.

References

1. Costa ACFM, Tortella E, Morelli MR, Kiminami RHGA. Synthesis, microstructure and magnetic properties of Ni–Zn ferrites. J Magn Magn Mater. 2003;256:174–82.
2. Eftekhari A, Molaei F, Arami H. Flower-like bundles of ZnO nanosheets as an intermediate between hollow nanosphere and nanoparticles. Mater Sci Eng: A. 2006;437:446–50.
3. Illy-Cherrey S, Tillement O, Dubois JM, Massicot F, Fort Y, Ghanbaja J, et al. Synthesis and characterization of nano-sized nickel(II), copper(I) and zinc(II) oxide nanoparticles. Mater Sci Eng: A. 2002;338:70–5.
4. More A, Verenkar VMS, Mojumdar SC. Nickel ferrite nanoparticles synthesis from novel fumarato-hydrazinate precursor. J Therm Anal Calorim. 2008;94:63–7.
5. Randhawa BS, Kaur M. A comparative study on the thermal decomposition of some transition metal maleates and fumarates. J Therm Anal Calorim. 2007;89:251–5.
6. Carp O, Segal E, Brezeanu M, Barjega R, Staniac N. Nonconventional methods for obtaining hexaferrites. J Therm Anal Calorim. 1997;50:125–35.
7. Bakalova A. Thermal and spectroscopic investigation of new binuclear Pt(II) complexes with carboxylic acids. J Therm Anal Calorim. 2009;96:593–7.
8. Logvinenko VA. Thermoanalytical approach to the study of the kinetic and thermodynamic stability of coordination compounds and clathrates. J Therm Anal Calorim. 1990;36:1973–80.
9. Stefanescu M, Sasca V, Birzescu M. Thermal behaviour of the homopolynuclear glyoxylate complex combinations with Cu(II) and Cr(III). J Therm Anal Calorim. 2003;72:515–24.
10. Kingsley JJ, Patil KC. A novel combustion process for the synthesis of fine particle α-alumina and related oxide materials. Mater Lett. 1988;6:427–32.
11. Deka S, Joy PA. Characterization of nanosized NiZn ferrite powders synthesized by an autocombustion method. Mater Chem Phys. 2006;100:98–101.
12. Hwang C-C, Tsai JS, Huang T-H. Combustion synthesis of Ni–Zn ferrite by using glycine and metal nitrates—investigations of precursor homogeneity, product reproducibility, and reaction mechanism. Mater Chem Phys. 2005;93:330–6.
13. Mangalaraja RV, Ananthakumar S, Manohar P, Gnanam FD. Initial permeability studies of Ni–Zn ferrites prepared by flash combustion technique. Mater Sci Eng: A. 2003;355:320–4.
14. Sorescu M, Diamandescu L, Peelamedu R, Roy R, Yadoji P. Structural and magnetic properties of NiZn ferrites prepared by microwave sintering. J Magn Magn Mater. 2004;279:195–201.
15. Anil Kumar PS, Shrotri JJ, Kulkarni SD. Low temperature synthesis of $Ni_{0.8}Zn_{0.2}Fe_2O_4$ powder and its characterization. Mater Lett. 1996;27:293–6.
16. Wu KH, Chang YC, Chang TC. Effects of SiO_2 content and solution pH in raw materials on Ni–Zn ferrite magnetic properties. J Magn Magn Mater. 2004;283:380–4.
17. Abdeen AM. Electric conduction in Ni–Zn ferrites. J Magn Magn Mater. 1998;185:199–206.
18. Arshak KI, Ajina A, Egan D. Development of screen-printed polymer thick film planner transformer using Mn–Zn ferrite as core material. Microelectron J. 2001;32:113–6.
19. Bhise BV, Dongare MB, Patil SA. X-ray infrared and magnetization studies on Mn substituted Ni-Zn ferrites. J Mater Sci Lett. 1991;10:922–4.
20. Caizer C, Ştefănescu M. Magnetic characterization of nanocrystalline Ni–Zn ferrite powder prepared by the glyoxylate precursor method. J Phys D. 2002;35:3035–40.
21. Niculescu M, Vaszilcsin N, Bîrzescu M, Budrugeac P, Segal E. Thermal and structural investigation of the reaction between 1,2-propanediol and $Ni(NO_3)2.6H_2O$. J Therm Anal Calorim. 2001;63:181–5.
22. McMorn P, Roberts G, Hutchings GJ. Oxidation of glycerol with hydrogen peroxide using silicalite and aluminophosphate catalysts. Catal Lett. 1999;63:193–7.
23. Nakamoto K. Infrared spectra of inorganic and coordination compounds. New York: Wiley; 1970. pp. 201, 199, 159, 217.
24. Prasad R, Sulaxna, Kumar A. Kinetics of thermal decomposition of iron(iii) dicarboxylate complexes. J Therm Anal Calorim. 2005;81:441–50.
25. Dranca I, Lupascu T, Sofransky V, Popa V, Vass M. Thermoanalytical study of some salts of 3d metals with d-tartaric acid. J Therm Anal Calorim. 1996;46:1403–12.
26. Zelenak V, Vargova Z, Gyoryova K. Correlation of infrared spectra of zinc(II) carboxylates with their structures. Spectrochim Acta A. 2007;66:262–72.
27. Stefanescu M, Stefanescu O, Stoia M, Lazau C. Thermal decomposition of some metalorganic precursors: Fe_2O_3 nanoparticles. J Therm Anal Calorim. 2007;88:27–32.
28. Suryanarayana C, Grant Norton M. X-ray diffraction. A practical approach. New York, London: Plenum Press; 1998.
29. JCPDS—International Center for Diffraction Data; 1999.